

Methylene Methanedisulfonate (MMDS) as a Novel SEI Forming Additive on Anode for Lithium Ion Batteries

Shaowei Mai, Mengqing Xu^{*}, Yating Wang, Xiaolin Liao, Haibin Lin, Weishan Li^{*}

School of Chemistry and Environment, Key Laboratory of Electrochemical Technology on Energy Storage and Power Generation of Guangdong Higher Education Institutes, Engineering Research Center of Materials and Technology for Electrochemical Energy Storage (Ministry of Education), South China Normal University, Guangzhou 510006, China

^{*}E-mail: mqxu@scnu.edu.cn (M. Xu), liwsh@scnu.edu.cn (W. Li)

Received: 25 May 2014 / Accepted: 20 August 2014 / Published: 25 August 2014

In this paper, methylene methanedisulfonate (MMDS) is reported as a novel solid electrolyte interphase (SEI) forming additive in propylene carbonate (PC) based electrolyte on graphite anode for lithium ion batteries. The effects of MMDS with PC-based electrolyte system of the electrochemical behaviors on graphite anode are investigated via combination of multi electrochemical methods, including charge/discharge test, cyclic voltammetry (CV), electrochemical impedance spectroscopy (EIS), and computation. Theoretical calculation result indicates that MMDS is preferably reduced on graphite to PC solvent, which is further supported by the CV experimental results. Charge-discharge test of Li/MCMB half cells and MCMB/LiMn₂O₄ full cells verify that the use of MMDS can successfully suppress the decomposition of PC and exfoliation of graphite. EIS technique is employed to monitor the SEI forming processes, indicating effective surface layer is formed on the graphite anode with incorporation of MMDS in PC-based electrolyte. The morphology, structure, and chemical nature of the formed SEI via MMDS participating are investigated by ex-situ analytical techniques, including SEM, TEM/EDS, and FTIR/ATR.

Keywords: Methylene methanedisulfonate; propylene carbonate; solid electrolyte interphase; lithium-ion batteries

1. INTRODUCTION

Lithium ion batteries (LIBs) have been extensively used for portable electronic devices and energy storage due to many merits such as high energy density and power capability [1]. A practical lithium ion battery consists of graphite anode, transition metal oxide (such as LiCoO₂, LiMn₂O₄ or LiNiO₂) cathode, and non-aqueous organic electrolyte. The electrochemical performance of lithium ion battery is highly dependent on the nature of electrolyte, such as power capability, high-low

temperature performance, and safety as well. Propylene carbonate (PC) is an attractive candidate as a solvent for nonaqueous electrolyte in LIBs due to its unique properties, such as low melting point, high dielectric constant, and wide electrochemical window [2,3]. However, PC-based electrolyte does not favor of forming protective surface layer on graphite anode electrode, which causes PC continuous decomposition on the surface and exfoliation of graphite, resulting in the failure of the cell [2,3]. To achieve the benefits of PC solvent while using in the electrolyte as co-solvent, many efforts have been devoted to solve this problem [3-6]. One of the most economical and effective methods is the incorporation of the SEI-forming additives [3-6], which can be reduced on the graphite anode before the PC decomposition/co-intercalation during the first forming cycle [7].

Sulfur-based compounds have been widely investigated as the SEI-forming additives, including ethylene sulfite (ES) [4], propylene sulfite (PS) [5] and vinyl ethylene carbonate (VES) [3]. Those additives have been verified to prevent the intercalation of PC into the graphite anode, but they also have their own drawbacks. Methylene methanedisulfonate (MMDS), which is composed of two $-O-S(=O)_2-$ units, has been proposed as electrolyte additive to improve the high-voltage cycling performance. Zuo et al recently reported MMDS could be preferably oxidized to form a cathode/electrolyte interphase layer on Li_xCoO_2 surface at high voltage, preventing carbonate solvents from continuous oxidization, and thus improved the cycling performance of graphite/ Li_xCoO_2 battery [8]. The authors claimed that the improved cycling performance at high-voltage only comes from the better surface layer formed on cathode electrode. While in terms of our recent experimental results, we believe that the benefits of incorporation MMDS on anode interphase may account for the enhanced cycling performance of graphite/ Li_xCoO_2 cell as well. In addition, to our knowledge, no research work has been reported based on the SEI-forming effects of MMDS on the anode electrode.

In this work, the electrochemical behavior and reduction mechanism of MMDS as a SEI-forming additive on graphite are illustrated. The reduction capability of MMDS and PC on graphite was investigated by density functional theory (DFT) computation and cyclic voltammetry (CV). The charge/discharge behaviors of Li/MCMB half cells and MCMB/ $LiMn_2O_4$ full cells were evaluated to determine the effects of MMDS on the decomposition and co-intercalation of PC into graphite anode. The process of SEI formation was monitored by using electrochemical impedance spectroscopy. The morphology, structure, and chemical nature of the formed SEI via MMDS participating were investigated by ex-situ analytical techniques, including SEM, TEM/EDS, and FTIR/ATR.

2. COMPUTATION AND EXPERIMENTAL

2.1. DFT calculations

The energy levels of the highest occupied molecule orbital (HOMO) and the lowest unoccupied molecule orbital (LUMO) of the electrolyte solvents and the additive MMDS were calculated by using Gaussian 03 programs package. The equilibrium and transition structures were fully optimized by B3LYP method at 6-31+G (d, p) basis set.

2.2. Material preparation and electrochemical characterization

Battery-grade carbonates solvents and lithium hexafluorophosphate (LiPF_6) were obtained from Guangzhou Tinci Materials Technology Co., Ltd. Methylene methanedisulfonate (MMDS) was purchased from Fujian Chuangxin Technology Co. with a purity of higher than 99%. The composition of the baseline electrolyte is 1.0 M LiPF_6 -PC/DEC (1:1, by weight). The graphite electrode was prepared with the mixture of 90 wt% mesocarbon micronbeads (MCMB) and 10 wt% PVDF coated on Cu foil. The LiMn_2O_4 electrode was prepared with the mixture of 90 wt% LiMn_2O_4 (Posco ES Material Co., LTD, Korea) and 10 wt% PVDF binder coated on Al foil. The mixed slurry was dried in vacuum oven overnight for further use.

Electrochemical studies were carried out on 2025-type coin cells consisting of a graphite electrode, a lithium foil and a Celgard 2400 separator. Similar coin-type full cells were assembled with LiMn_2O_4 as the positive electrode, MCMB as the negative electrode. The cells were fabricated in an argon-filled glove-box, in which the moisture and oxygen contents were maintained less than 1.0 ppm.

The Li/MCMB half cells were charged and discharged between 0.005 and 2.5 V at a constant-current rate of 0.1 C (1 C = 372 mA g^{-1}); the MCMB/ LiMn_2O_4 full cells were cycled between 2.5 and 4.3 V at 0.2 C (1 C = 148 mA g^{-1}) current rate. They were carried out on LAND test system (Land CT2001A, China) at 25 °C. Cyclic voltammetry (CV) of Li/MCMB half cells was performed on electrochemical station (Autolab, Metrohm Co., Switzerland) in the potential range of 0.005-2.5 V at a scan rate of 0.2 mV s^{-1} . Electrochemical impedance spectra (EIS) were measured on electrochemical station, the AC perturbation was ± 10 mV, and the frequency range was from 10^5 Hz to 10 mHz.

2.3. Surface analysis

The cycled MCMB/ LiMn_2O_4 cells were disassembled in the Ar-filled glove box and the electrodes were rinsed with DMC solvent, followed by vacuum drying overnight before analysis. The surface morphology, structure, and composition of the cycled electrodes with and without the addition of MMDS were inspected by scanning electron microscopy (SEM, JSM-6510, JEOL Co., Japan), and transmission electron microscopy (TEM, JEM-2100, JEOL Co., Japan) equipped with an energy dispersive spectroscopy (EDS) detector. Each surface organic functional group was characterized by Fourier transform infrared spectroscopy (FTIR) (Bruker Tensor 27) instrument within 600-4000 cm^{-1} .

3. RESULTS AND DISCUSSION

3.1. DFT calculations

The HOMO and LUMO energy levels of PC and MMDS were calculated based on B3LYP/6-311+G (d) level, as depicted in Table 1. The obtained HOMO energy levels are -8.6481 and -9.3167 eV for PC and MMDS, respectively. The LUMO energy of MMDS is -1.2077 eV, which is much lower than that of PC (-0.1742 eV). Based upon molecular orbital theory, a molecule with a lower

energy level of LUMO should be a better electron acceptor and more reactive on the negatively charged surface of the anode. Therefore, MMDS will be reduced prior to PC during the first charge process. The electrochemical experiments are consistent with the computational results, as discussed below.

Table 1 The HOMO and LUMO energy levels of PC and MMDS.

Molecule	HOMO (eV)	LUMO (eV)
PC	-8.6481	-0.1742
MMDS	-9.3167	-1.2077

3.2. Charge-discharge test

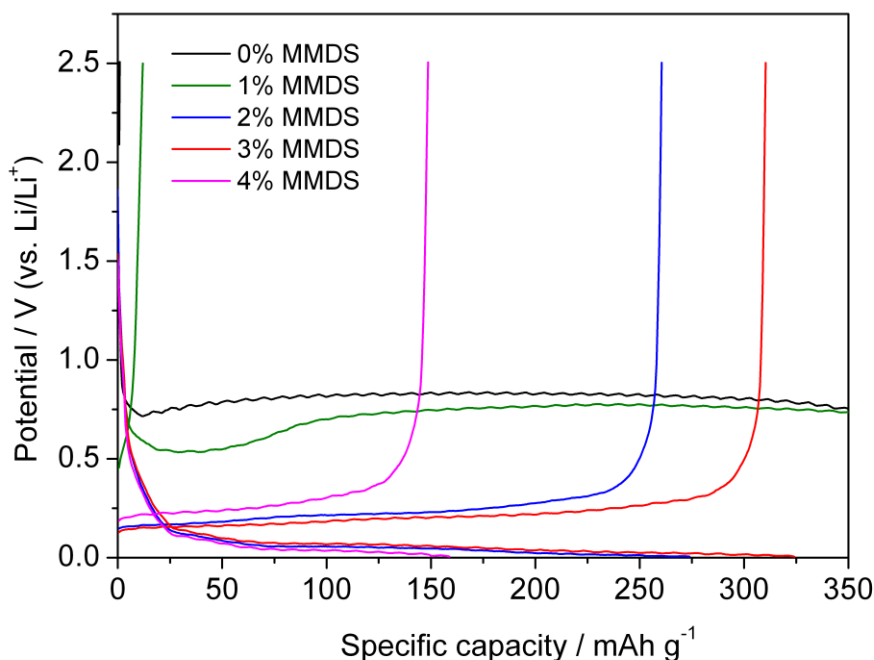


Figure 1. First charge/discharge curves of Li/MCMB half cells using baseline electrolyte with various contents of MMDS. The cells were cycled between 2.5-0.005 V at a scan rate of 0.1 C (1 C = 372 mA g⁻¹).

The effect of MMDS content on the performance of the graphite anode was considered with Li/MCMB half cells. Fig.1 presents the charge/discharge curves of Li/MCMB half cells using 1.0 M LiPF₆-PC/DEC (1:1, by weight) electrolytes with various contents of MMDS, and the corresponding coulomb efficiency is depicted in Table 2.

Table 2. Parameters of the first charge-discharge of Li/MCMB half cells with various contents of MMDS.

Content	Charge capacity (mAh g ⁻¹)	Discharge capacity (mAh g ⁻¹)	Coulomb efficiency (%)
0% MMDS	459.0	0.9	0.2
1% MMDS	610.5	12.0	2.0
2% MMDS	273.9	260.6	95.1
3% MMDS	324.2	310.4	95.7
4% MMDS	158.9	148.6	93.5

For the baseline electrolyte (0% MMDS), there is a long plateau at about 0.75 V (vs. Li/Li⁺) for the charge process, which is attributed to the PC decomposition and co-intercalation of PC with Li-ions into graphite [2,3]. The decomposition and co-intercalation of PC result in the exfoliation of graphite, which thus led to no reversible de-intercalation of lithium ions from graphite electrode occurring for the discharge process. With using less than 2 wt% MMDS, only very small reversible capacity can be recorded, indicating that low content of MMDS fails in forming a protective SEI on graphite. While with using over 2 wt% MMDS, the typical plateaus for the lithium intercalation/de-intercalation are observed below 0.25 V (vs. Li/Li⁺), suggesting effective SEI is formed on the graphite electrode thus allowed reversible intercalation/de-intercalation of lithium ions electrochemical processes taking place. Surprisingly, it can be noted that larger content of MMDS (4 wt%) yields a negative effect on the graphite performance. This phenomenon may be ascribed to the thicker SEI formed on the graphite surface, resulting in higher interfacial impedance of the electrode. With the highest discharge capacity and coulomb efficiency (310.4 mAh g⁻¹ and 95.7%), the optimal content of MMDS for the SEI formation is considered to be 3 wt%.

Fig.2 compares the charge/discharge profiles of MCMB/LiMn₂O₄ cells without and with 3% MMDS containing electrolyte. Fig.2 (a), related to the MMDS-free electrolyte, shows a continuous charging behavior, suggesting the failure of the cell upon cycling. The long-term charging plateau observed here can be ascribed to the continuous decomposition of PC at 0.75 V on graphite electrode, and thus the cell could not reach the upper cut-off voltage, 4.3 V (vs. Li/Li⁺). However, with regards to the cell with 3% MMDS containing electrolyte, typical charge/discharge profiles were observed upon cycling, with cycling coulombic efficiency of 50.6%, 89.4%, and 91.5%, respectively, for the first three cycles, suggesting a protective surface film is formed on the graphite electrode in PC-based electrolyte with MMDS incorporation.

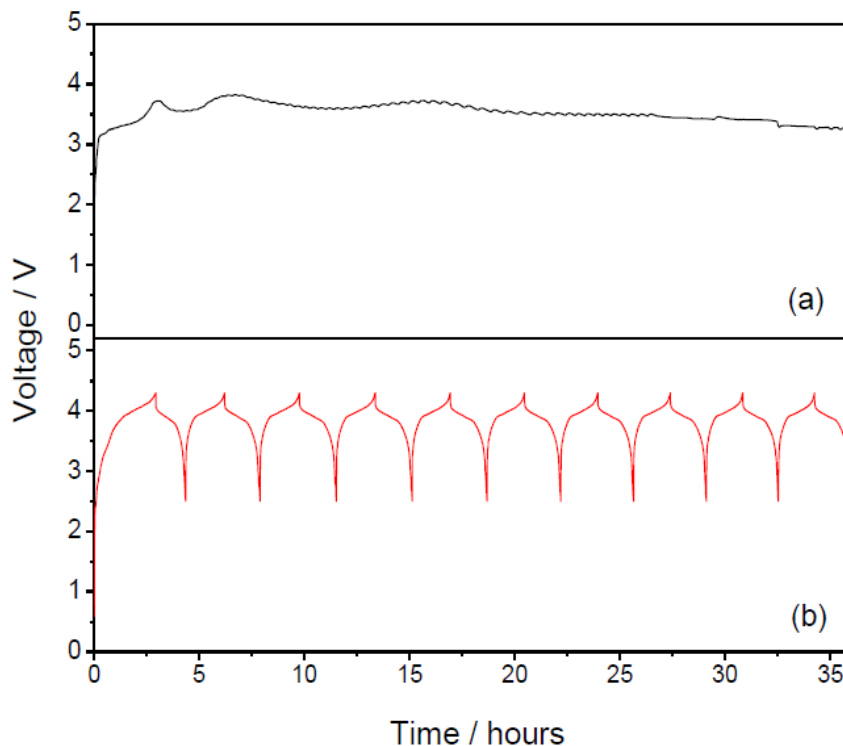


Figure 2. Charge/discharge profiles of MCMB/LiMn₂O₄ cells in repeated galvanostatic cycling at room temperature, 0.2 C, without (a) and with (b) 3 wt% MMDS in the electrolytes.

3.3. Cyclic voltammetry measurements

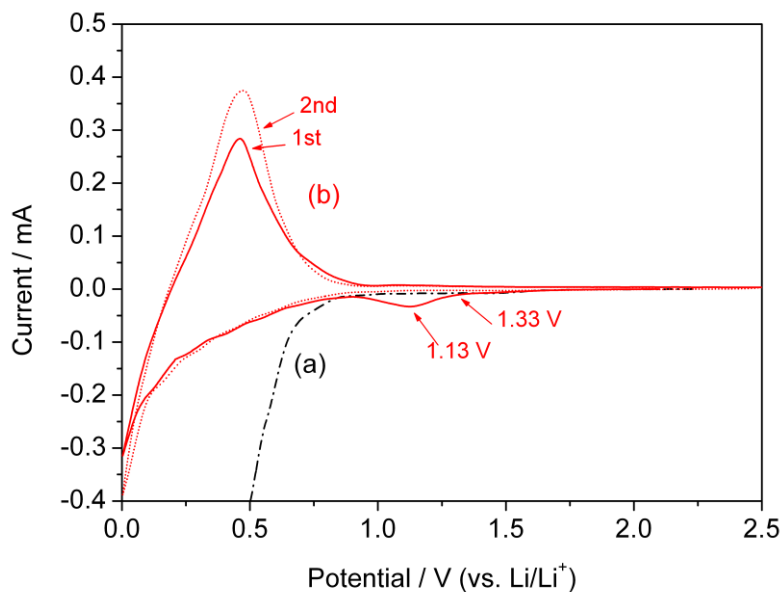


Figure 3. (a) Cyclic voltammograms of MCMB electrodes in 1.0 M LiPF₆-PC/DEC (1:1, by weight) electrolyte without (a) and with (b) 3 wt% MMDS, scan rate: 0.2 mV s⁻¹.

Fig.3 displays the cyclic voltammograms of MCMB electrodes in 1.0 M LiPF₆-PC/DEC electrolyte without and with 3% MMDS added. The CV profiles clearly show the effect of MMDS

additive, which effectively suppresses the decomposition and co-intercalation of PC. In the electrolyte without MMDS, as shown in Fig. 3a, the decomposition of PC begins at around 0.75 V (vs. Li/Li⁺) [9] and the cathodic current becomes much larger in the lower potential direction, and eventually, no anodic peak corresponding to Li⁺ de-intercalation was observed during reversed scanning. However, as respect to the electrolyte with 3% MMDS added, different electrochemical behavior was observed. Reversible anodic peak appeared upon reversed scans, suggesting reversible electrochemical processes of lithium ions intercalation and de-intercalation taking place with MMDS presence electrolyte. In addition, small reduction peak at 1.33 V vs. Li/Li⁺ was observed in the first scan and disappeared in the second cycle for the electrolyte with MMDS added. We believe that this peak is ascribed to the reduction of MMDS on MCMB electrode and forms a protective surface layer, which allows the reversible intercalation and de-intercalation of lithium ions occurring in PC-based electrolyte system. The higher reductive capability of MMDS on graphite anode observed here is consistent with the DTF calculation results as we discussed above.

3.4. Electrochemical impedance spectra (EIS)

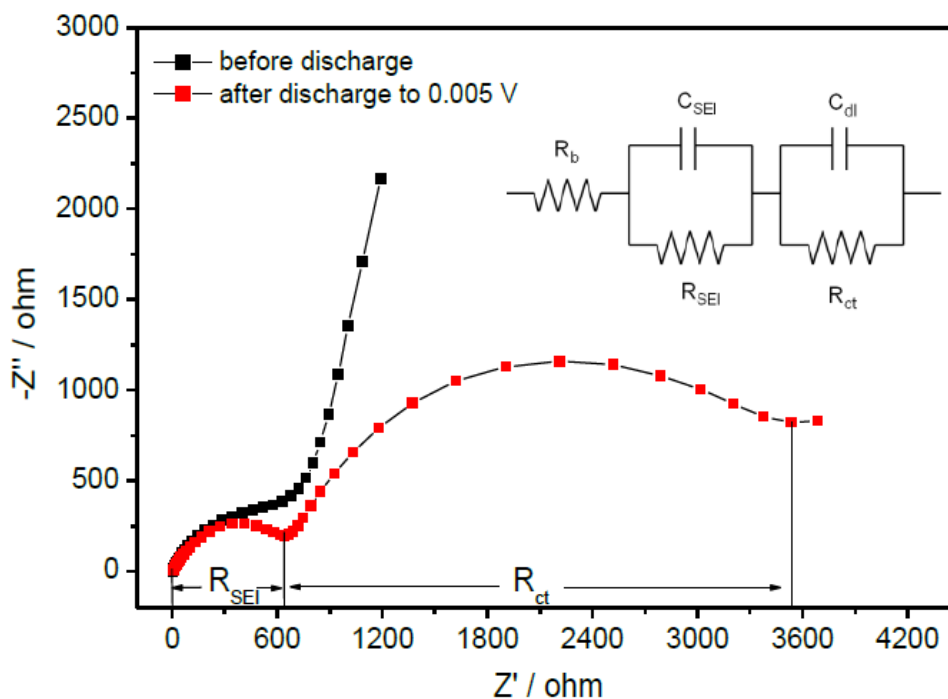


Figure 4. Electrochemical impedance spectra with an equivalent circuit of Li/MCMB cell with 3 wt% MMDS in the electrolyte before and after charging to 5 mV.

The process of SEI formation was monitored by using electrochemical impedance spectroscopy. Fig.4 shows the Nyquist plots of the Li/MCMB cell with 3 wt% MMDS in the electrolyte, before and after the first charging to 5 mV under the scan rate of 0.2 mV s⁻¹. From Fig.3 we can see that the impedance plot after the first charge to 5 mV exhibits two depressed semi-cycles in the medium and low frequency range. The inset equivalent circuit was used to analyze the

electrochemical cell impedance spectra. R_b is the total resistance of electrolyte + electrode + separator, while R_{SEI} and C_{SEI} are the resistance and capacitance of the SEI film formed on the surface of the electrode, respectively; R_{ct} and C_{dl} represent the charge-transfer resistance and double layer capacitance, respectively [10]. For the electrode in the MMDS-containing electrolyte, the R_{SEI} impedance can be seen after the first charge to 5 mV, suggesting a SEI film was formed on the graphite. This result supports the fact that MMDS can be reduced to form a SEI film on graphite during the first discharge process, as seen in Fig.3.

3.5. SEI analysis

In order to understand the nature of the SEI formed by MMDS, the surface chemistry of cycled electrodes was analyzed with SEM, TEM/EDS, and FTIR measurements. Fig.5 shows the SEM images of the MCMB electrode surface before and after cycling in 1.0 M LiPF_6 -PC/DEC electrolyte with and without MMDS. Before cycling, the surface of the original MCMB is smooth and clean, as shown in Fig.5 (a, b). After cycling in the baseline electrolyte, Fig.5 (c, d), it can be seen that the surface of MCMB is rough and corroded, which indicates that the bulk structure of the MCMB electrode is destroyed, due to the co-intercalation of PC with solvated lithium ions. As regards to the electrolyte cycling in MMDS containing electrolyte, the fresh flake-shaped particles are dulled and covered by precipitates, as clearly presented in Fig. 5e and 5f, which are corresponding to the reduced decomposition products of MMDS on graphite anode surface.

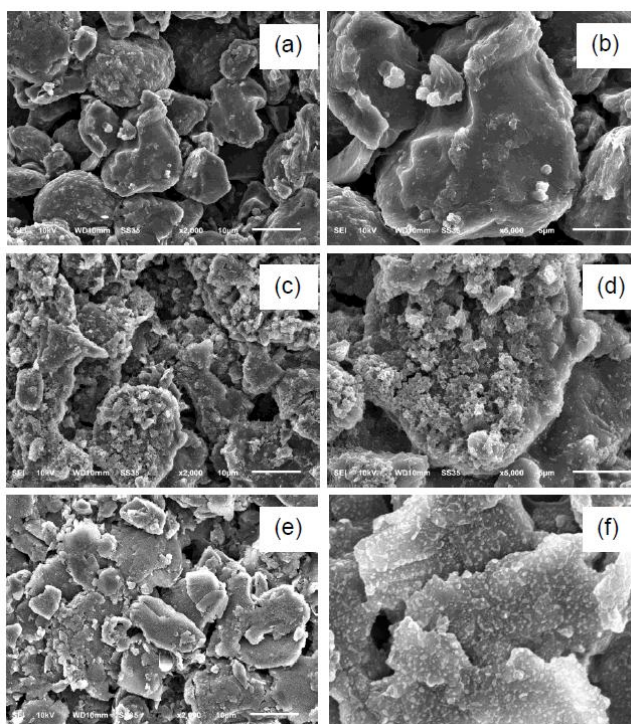


Figure 5. SEM images of MCMB electrode obtained before cycling (a,b), after cycling in 1.0 M LiPF_6 -PC/DEC (1:1, by weight) electrolyte without additive (c,d) and with 3 wt% MMDS (e,f).

To better understand the structure and composition of the SEI formed on the MCMB anode surface in PC-based electrolyte system with 3% MMDS containing, the cycled MCMB electrode was analyzed with TEM and EDS. The TEM image and related EDS pattern of the electrode are depicted in Fig. 6. A thin layer, about 200 nm thickness, covering the MCMB particle is observed in Fig. 6a, suggesting an effective SEI is formed on the surface of graphite particles, which facilitates the reversible intercalation/de-intercalation of lithium ion processes. From the EDS spectrum, as shown in Fig. 6b, a sulfur peak at 2.3 keV was detected on the MCMB surface. Apparently, this peak corresponds to sulfur in the sulfite compounds formed on the MCMB electrode surface during the reduction of MMDS. This suggests that the reductive products of MMDS take part in the formation of the SEI layer. Hence, it is believed that the reduction of MMDS assists in forming a SEI layer on the graphite electrode, and then prevents the PC decomposition and the exfoliation of graphite.

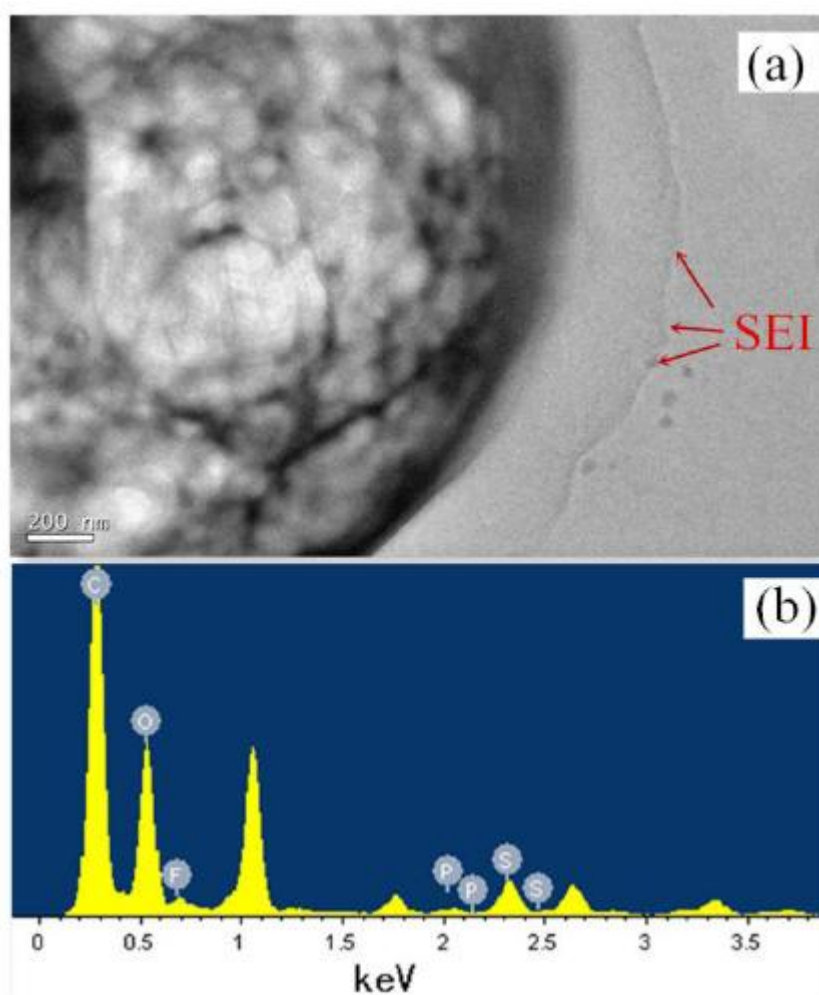


Figure 6. TEM image (a) and EDS pattern (b) of MCMB electrode after cycling in 1.0 M LiPF₆-PC/DEC (1:1, by weight) electrolyte with 3 wt% MMDS.

FTIR-ATR was used to further investigate the chemistry composition of the SEI formed on MCMB electrode with MMDS-containing electrolyte, and baseline electrolyte. Fig.7 presents the FTIR spectra of the MCMB electrodes before and after cycling in the electrolytes with and without 3 wt%

MMDS. For the fresh MCMB electrode, the main absorption peaks are predominant by PVDF binder, which is characteristic at 1392.5, 1176.5 and 817.8 cm^{-1} [2]. After cycling in the baseline electrolyte, a number of new absorption bands corresponding to the decomposition products of solvents (PC or DEC) can be observed. The peaks located at 1726.2 cm^{-1} (C=O) 833.2 cm^{-1} (OCO_2/CO_3) and 1444.0 cm^{-1} (CH_2) are attributed to ROCO_2Li or $(\text{CH}_2\text{OCO}_2\text{Li})_2$ [2,11]. Significant absorption peaks at 1031.9 cm^{-1} and 1182.3-1228.6 cm^{-1} (SO_3) appear on the electrode cycled in the MMDS-containing electrolyte. These absorptions correspond to ROSO_2OR [11,12], which should be the reduction product of MMDS, and confirms that the reduction products of MMDS are incorporated into the SEI formed on graphite.

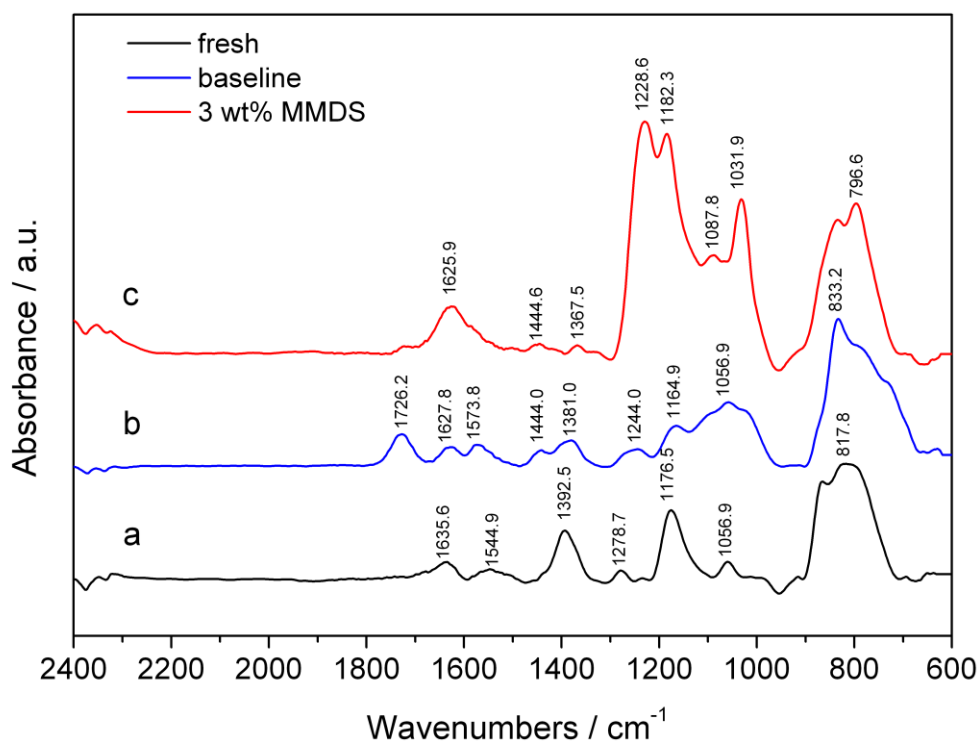


Figure 7. FTIR spectra of MCMB electrodes before and after cycling in the baseline electrolyte and the MMDS-containing electrolyte.

4. CONCLUSIONS

Methylene methanedisulfonate (MMDS) is firstly evaluated as a SEI forming additive in propylene carbonate (PC) based electrolyte for lithium ion batteries. Addition of 3 wt% MMDS in the PC-based electrolyte, Li/MCMB half cells and MCMB/ LiMn_2O_4 full cells can be successfully charged-discharged with high coulombic efficiency. This is ascribed to the effective SEI film formed on graphite in the presence of MMDS, preventing the decomposition of PC and the subsequent exfoliation of graphite. The effect of MMDS on the formation of SEI on MCMB anode was

understood by DFT, CV, EIS, SEM, TEM, EDS and FTIR measurements. It was found that MMDS can be reduced prior to PC, forming a SEI layer on graphite, and thus prevents the decomposition and co-intercalation of PC.

ACKNOWLEDGEMENTS

This research work is supported by the National Natural Science Foundation of China (Nos: 21373092, 21273084), the Joint Project of National Natural Science Foundation of China and Natural Science Foundation of Guangdong (No.U1134002), Natural Science Foundation of Guangdong Province (10351063101000001).

References

1. K. Xu, *Chem. Rev.*, 104 (2004) 4303
2. B. Li, M.Q. Xu, T.T. Li, W.S. Li, S.J. Hu, *Electrochem. Commun.*, 17 (2012) 92
3. W. H. Yao, Z.R. Zhang, J. Gao, J. Li, J. Xu, Z.C. Wang, Y. Yang, *Energy Environ. Sci.*, 2 (2009) 1102
4. H. Wroding, J.Q. Besenhard, M. Winter, *J. Electrochem. Soc.*, 146 (1999) 470
5. G. H. Wroding, T.M. Wroding, J.Q. Besenhard, M. Winter, *Electrochem. Commun.*, 1 (1999) 148
6. R. McMillan, H. Slegel, Z.X. Shu, W. Wang, *J. Power Sources*, 81 (1999) 20
7. S. S. Zhang, *J. Power Sources*, 162 (2006) 1379
8. X. X. Zuo, C.J. Fan, X. Xiao, J.S. Liu, J.M. Nan, *J. Power Sources*, 219 (2012) 94
9. R. Wagner, S. Brox, J. Kasnatscheew, D. R. Gallus, M. Amereller, I. C. Laskovic, M. Winter, *Electrochem. Commun.*, 40 (2014) 80
10. D. S. Lu, W. S. Li, X. X. Zuo, Z. Z. Yuan, Q. M. Huang, *J. Phys. Chem. C*, 111 (2007) 12067
11. P. Verma, P. Maire, P. Novák, *Electrochim. Acta*, 55 (2010) 6332
12. Felix, J.-H. Cheng, S. Hy, J. Rick, F.-M. Wang, B.-J. Hwang, *J. Phys. Chem. C*, 117 (2013) 22619

© 2014 The Authors. Published by ESG (www.electrochemsci.org). This article is an open access article distributed under the terms and conditions of the Creative Commons Attribution license (<http://creativecommons.org/licenses/by/4.0/>).